LITHOSPHERE (RUSSIA), 2018, volume 18, No. 5A, pp. 20–36

MURZINKA MASSIF IN THE MIDDLE URALS AS AN EXAMPLE OF AN INTERFORMATIONAL GRANITE PLUTON: MAGMATIC SOURCES, GEOCHEMICAL ZONATION, PECULIARITIES OF FORMATION

German B. Fershtater, Nadezhda S. Borodina

Zavaritsky Institute of Geology and Geochemistry, UB RAS, 15 Akad. Vonsovsky St., Ekaterinburg, 620016 Russia, e-mail: gerfer@online.ural.ru

Received 08.11.2017, accepted 07.05.2018

Murzinka massif constitutes an interformational sheet-like body reaching up 6 km in length steeply dipping to the east. Proterozoic metamorphic rocks of predominantly granulite facies (P = 5–6 kbar, T = 750–800°C) occur at the base of the massif, with Silurian-Devonian volcanic-sedimentary rocks metamorphosed in the epidote-amphibolite facies occurring in its roof. The petrogenic elements were determined at the Laboratory for Physicochemical Research Methods of the Zavaritsky Institute of Geology and Geochemistry, UB RAS. The content of trace elements was determined at the laboratories of the University of Granada in Spain and at the Institute of Geology and Geochemistry using the ICP-MS method. In the eastern direction, the rocks change their composition from predominantly basic to granitoid as they approach the massif. The gneisses of the granitoid composition experienced a high degree of melting; the anatectic melt formed the western part of the Murzinka massif. The granites form three complexes: 1) Yuzhakovo – veins of biotite orthoclase antiperthite granites varying in K_2O content in the metamorphic rocks of the base of the massif; 2) Vatikha – biotite orthoclase antiperthite granites making up the western part of the Murzinka massif; 3) Murzinka – two-mica predominantly microcline granites occurring in the eastern part of the massif. Vatikha and Murzinka granites have the same isotopic age (about 255 Ma). A clear geochemical zonation is revealed in the massif: from west to east (from the base to the roof), the contents of Rb, Li, Nb, Ta increase in the granites of the Vatikha and Murzinka complexes. In the same direction, the ratios K/Rb, Zr/Hf, Nb/Ta decrease, as well as the contents of Ba and Sr. Naturally, the compositions of such rock-forming minerals as plagioclase and biotite also change. The isotopic characteristics of the granites of the Vatikha (Sr_i = 0.70868–0.70923 and εNd_{255} from –8.9 to –11.9) and Murzinka (Sr_i = 0.70419–0.70549, εNd_{255} from –2.6 to +2.3) complexes suggest that the substratum of the former was represented by Proterozoic granite-gneisses, whereas the rocks of the newly formed crust, possibly similar to the Silurian-Devonian volcanogenic-sedimentary rocks, which are at contact with the Murzinka granites, served as the substrate for the latter.

Keywords: *granites, geochemical zonation, isotopic characteristics of granites, P-T parameters of granite magmatism*

Acknowledgments

The work was carried out within project No. 0393-2016-0020 of the state task of the IGG UB RAS, state registration number AAAA-A18-118052590029-6.

INTRODUCTION

The issue associated with the formation of granite massifs has always been at the forefront of attention of petrologists and geochemists. The use of modern analysis methods (including in-situ methods) combined with detailed geological observations allows us to approach the solution of such fundamental issues of granite formation as the duration and stages of the process, its physicochemical parameters, laws and conditions of granite formation and magmatic evolution, sources of granite magmas and fluids.

This article is aimed at considering these issues using the well-studied Murzinka massif (Middle Urals) as an example. The massif in question was described earlier in [Orogenic granitoid magmatism..., 1994]; however, new more accurate analytical data allow us to return to this unique subject matter.

The massif constitutes an interformational sheet-like body reaching up to 10 km in thickness dipping steeply to the east. It is overlain by presumably Devonian volcanic-sedimentary rocks and underlain by Proterozoic para- and orthorocks of the Murzinka-Aduy metamorphic complex (MMC) [Keil'man, 1974; Korovko, Dvoeglazov, 1986], intruded by numerous granite veins, which we identified in the Yuzhakovo complex (Fig. 1). The massif includes two isotopically coeval granite complexes. Its western part is composed of orthoclase, magnetite and biotite granites from the Vatikha complex, whereas the eastern part comprises microcline-orthoclase and microcline binary granites from the Murzinka complex [Orogenic granitoid magmatism..., 1994]. The veins of chamber pegmatites making up the famous Ural gemstone belt were formed in the bottom part of the massif [Fersman, 1940; Talantsev, 1988], with common pegmatites characterised by rare-metal mineralisation and various metasomatites being formed over its top.

METHODS

The petrogenic elements were determined at the Laboratory for Physicochemical Research Methods of the Zavaritsky Institute of Geology and Geochemistry,

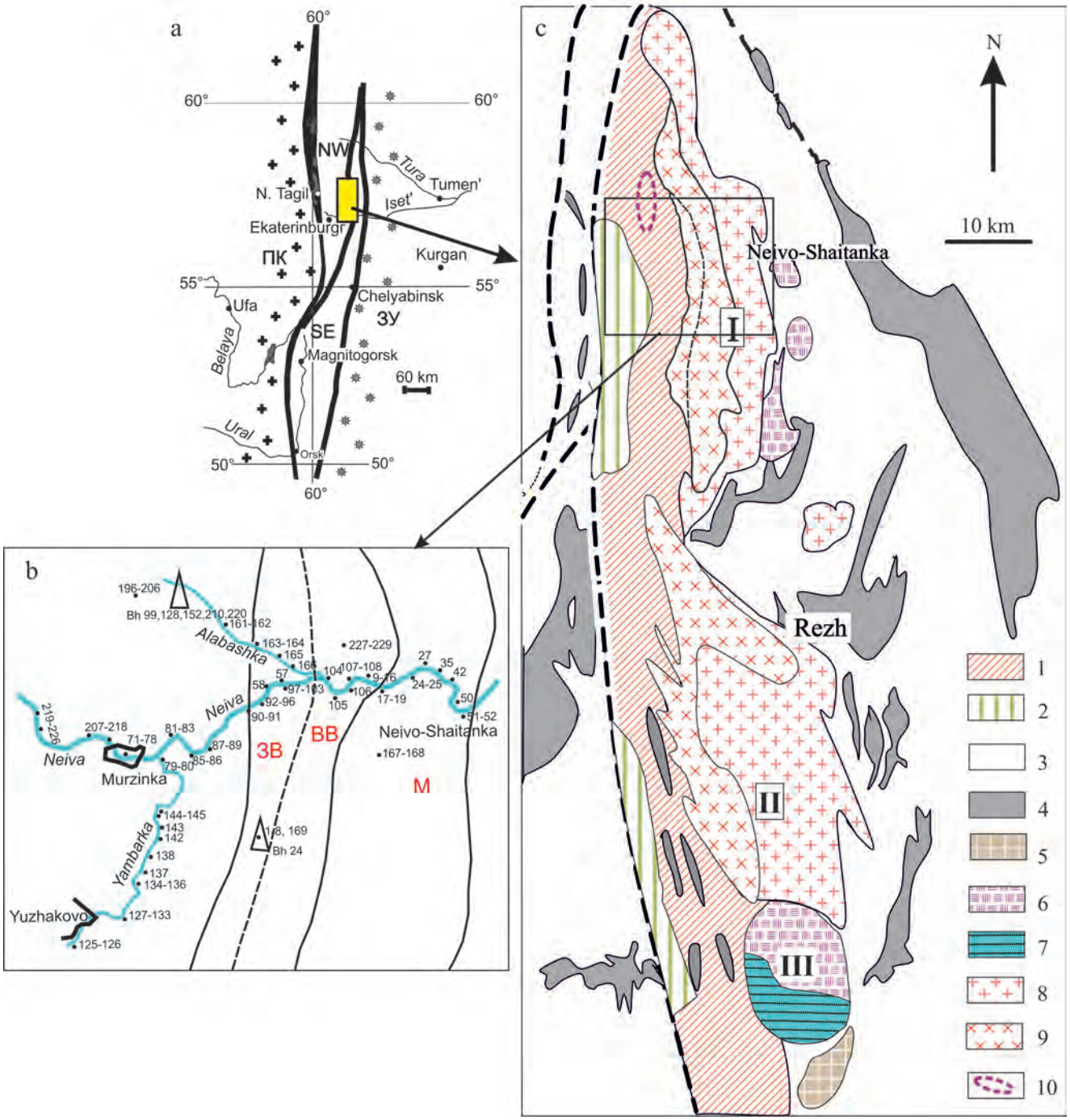

Fig. 1. Location of area under study.

a – the main geological structures of the Urals: ПК – paleocontinental sector, ЗУ – Trans-Urals, СЗ and ЮВ – island arc-continental megablocks [Fershtater, 2013]. b – a scheme of the placement of Murzinka rock samples mentioned in the text, the contours of the Murzinka massif and approximate areas of the granites of the West Vatikha (WV), East Vatikha (EV) subcomplexes and the Murzinka (M) complex. c – a schematic geological map of Murzinka (I), Aduy (II) and Kamensk (III) massifs, compiled on the basis of the geological map of the Urals, ed. by I.D. Sobolev with authors' changes.
1, 2 – rocks of the Murzinka-Aduy metamorphic complex: 1 – biotite ortho- and paragneisses with interbedded marbles, 2 – high-aluminum ortho- and paragneisses of alkaline-mafic composition; 3 – Silurian-Devonian volcanic-sedimentary rocks; 4 – serpentinites; 5 – Early Devonian migmatised gabbros, trondhjemites and granodiorites; 6, 7 – Carboniferous tonalites, granodiorites and granites (6) and migmatites (7) in Kamensk massif; 8 – two-mica microcline-orthoclase granites, which presumably crystallised from magma formed by the migmatisation of Carboniferous tonalites and granodiorites (Murzinka complex); 9 – biotite antiperthite, essentially orthoclase granites with magnetite, presumably formed through the partial melting of ancient metamorphic strata (Vatikha complex – the dashed line roughly separates the granites of the West and East Vatikha subcomplexes); 10 – Alabashka chamber pegmatite field.

UB RAS (analysts N.P. Gorbunova, L.A. Tatarinova and G.S. Neupokoeva). The content of trace elements was determined at the laboratories of the University of Granada in Spain (analysts F. Bea, P. Montero) using the ICP-MS method and at the Institute of Geology and Geochemistry (analysts D.V. Kiseleva, N.V. Cherednichenko and L.K. Deryugina) using an emission spectral analysis. The accuracy of the analyses comes to 2 and 5 rel % for the concentrations of 50 ppm and 5 ppm, respectively.

Murzinka-Aduy metamorphic complex

At the latitude of the Murzinka granite massif, the rocks of the complex are represented by para- and orthogneisses, whose bulk composition varies from basic to granitoid. The western and central parts of the complex comprise gneisses of mainly basic composition, interstratified with more silicic rocks (Table 1, an. 1–8). In terms of mineral composition, high-alumina (see Table 1, an. 2, 3, 7, 8) and high-alkaline rocks (an. 1, 4–6) are distinguished. The former are represented by the alternation of biotite, biotite-garnet, biotite-cordierite-sillimanite and biotite-corundum gneisses with tourmaline. Corundum gneisses (an. 2) which are similar in terms of mineralogy to corundum syenites from the Ilmeny mountains described in [Levin et al., 1975; Popov, Popova, 1975]: well-formed corundum crystals (0.5–5 cm in size), whose arrangement does not correspond to the gneissic structure, are surrounded by antiperthite plagioclase and immersed in a biotite-plagioclase-quartz-corundum matrix, in which corundum grains are strictly oriented. High-alkaline gneisses are represented by biotite and clinopyroxene-hornblende-biotite varieties with antiperthite plagioclase An_{30-40} characteristic of all metamorphic rocks from the Murzinka complex, as well as a rich complex of accessory minerals: magnetite, sphene, apatite and allanite (see Table 1, an. 4, 5). In terms of mineral and chemical composition, these rocks are close to the so-called vaugnerites – potassium-rich basic and diorite rocks in the Western European variscites (Massif Central, France), which accompany the main phase of granite crust formation and reflect the contribution of the mantle to this process [Sabatier, 1980, 1991; Scarrow et al., 2009]. Researchers attribute the formation of vaugnerites to the most intense, ‘catastrophic’ melting of the crust [Couzinie et al., 2014].

In the area of the Alabashka pegmatite field (see Fig. 1), where many holes were drilled during exploration, the section of metamorphic rocks hosting pegmatite veins is represented by carbonate rocks (calciphyres) interstratified with biotite gneisses of predominately diorite composition and intruded by the granite and adamellite veins of the Yuzhakovo complex. The metamorphic paragenesis of calciphyres is as follows: calcite, dolomite, phlogopite, diopside and graphite; with the mineral composition of gneisses comprising biotite, hornblende, sometimes diopside and orthopyroxene, orthoclase, antiperthite plagioclase An_{40-60}, apatite, magnetite. Orthogneisses of diorite and more silicic composition predominate. Paragneisses are characterised by a thin-banded texture and low-strontium content. Granites intrude already metamorphosed rocks. They transect gneissic structures and contain the xenoliths of gneisses and calciphyres metamorphosed in the context of a granulite facies. Rocks that are in contact with the granite veins are skarnified. The following minerals are formed in them: forsterite, diopside porphyroblasts, bytownite An_{70-90}, scapolite, prehnite; phlogopite chloritises; apatite, sphene and sulphides (pyrite, chalcopyrite) occur in large quantities in them. The skarnification is of the bimetasomatic type, which is manifested in granites by the development of prehnite, scapolite and less commonly diopside. The thickness of endoskarn zones reaches 0.5 m. Unlike granites, chamber pegmatites (Mokrusha and other veins) do not affect the host rocks significantly and have well-defined boundaries with them, without there being any noticeable changes on both sides.

The mineral composition of MMC gneisses – a high titanium content (up to 5.5 wt % in biotite and up to 2 wt % in amphibole), as well as antiperthite plagioclase and poorly structured potassium feldspar – indicates high temperatures of mineral formation corresponding to the granulite facies [Orogenic granitoid magmatism..., 1994].

The easternmost part of the MMC was preserved only in the form of the xenoliths of granite gneisses in Vatikha granites (see Table 1, an. 9–11). The rocks experienced partial melting, whose products formed the western part of the Murzinska massif. The fact that the composition of restite is close to that of adamellite suggests that the composition of protolith was only slightly different from granite and experienced a high degree of partial melting.

The structure of the MMC exhibits latitudinal lateral zonation, which is characterised by an increase in the content of silica in metamorphic rocks from west to east (Fig. 2). This increase reflects the initial change in the composition of the rocks rather than granitisation, which is very weak. The use of some well-known discriminatory diagrams (Fig. 3) confirms the conclusion that rocks that served as the protolith of metamorphic rocks belong to a high-alkaline basalt-andesite series. In this connection, we should recall that G.A. Keil’man [1974] suggested that rocks of the Ilmeny complex constitute the southern continuation of the MMC. The presented data on the rock composition, as well as the presence of such specific gneisses in the MMC as corundum ones, which are not known anywhere in the Urals, except for the Ilmeny Mountains [Levin et al., 1975], confirm this assumption.

The U-Pb age of zircon from a typical biotite diorite gneiss, determined using both the classical method and the LA-ICP-MS, is more than 1600 Ma [Krasnobaev

Table 1. Content of petrogenic (wt %) and trace (ppm) elements in the metamorphic rocks of the Murzinka-Aduy complex

Element	1	2	3	4	5	6	7	8	9	10	11
SiO_2	49.30	51.64	54 00	55.34	57.17	62.50	66.49	67.66	67.61	69.00	70.15
TiO_2	2.31	1.12	0.92	1.47	0.90	0.98	0.63	0.85	0.47	0.36	0.26
Al_2O_3	17.91	26.83	16.47	18.19	18.53	16.09	14.35	13.25	16.20	15.55	14.66
Fe_2O_3	2.10	1.21	0.61	2.15	0.46	2.17	2.56	0.70	0.43	0.50	0.46
FeO	8.34	4.33	7.38	5.23	5.00	3.00	2.80	5.60	2.55	2.77	2.90
MnO	0.12	0.03	0.13	0.07	0.10	0.10	0.05	0.05	0.05	0.04	0.05
MgO	3.52	2.45	5	3.16	3.92	2.64	2.72	2.37	0.73	1.26	0.59
CaO	5.44	1.52	6.87	4.52	5.29	4.77	3.11	0.48	1.87	2.34	1.32
Na_2O	2.80	5.78	3.44	4.55	4.40	4.36	3.38	2.39	4.89	5.00	3.67
K_2O	3.95	3.67	3.2	2.75	2.39	2.00	2.41	5.30	3.26	2.18	4.65
P_2O_5	1.21	0.22	0.25	0.87	0.10	ND	ND	ND	0.17	0.14	0.13
Impurities	2.04	1.17	1.53	1.21	1.33	0.80	0.80	1.00	0.62	0.31	0.59
Σ	99.04	99.97	99.8	99.86	99.59	99.40	99.29	99.65	98.85	99.76	99.43
Li	18.88	73.86	ND	30.00	34.00	25.42	10.59	125.7	14.70	28.00	11.26
Rb	160.8	88.82	73.00	149.0	76.00	66.74	75.76	73.80	31.28	23.00	85.54
Cs	1.83	1.05	ND	2.00	3.00	2.05	1.49	2.32	0.81	1.00	0.62
Be	1.75	6.66	1.00	3.00	3.00	2.21	1.34	1.78	0.68	2.00	1.67
Sr	1370	43.82	460.0	0.00	398.0	345.1	406.1	70.81	745.95	368.0	224.2
Ba	2527	88.74	ND	0.00	431.00	358.8	413.1	185.6	2004.4	468.0	646.7
Sc	13.88	22.22	35.00	16.00	25.00	14.59	14.37	45.24	2.30	9.00	3.53
V	250.2	605.1	170.0	150.0	143.0	102.4	115.7	435.0	25.53	47.00	13.95
Cr	7.58	258.7	49.00	3.00	103.0	94.03	37.19	191.9	0.93	4.00	2.97
Co	17.46	39.74	24.00	15.00	21.00	16.83	13.82	24.80	2.97	5.00	2.16
Ni	18.18	56.31	24.00	18.00	55.00	124.9	22.11	57.32	1.89	2.00	2.44
Cu	28.87	35.19	ND	36.00	8.00	27.81	126.9	18.47	14.99	28.00	7.37
Zn	140.72	29.76	ND	143.0	76.00	64.35	57.18	83.68	60.49	54.00	46.34
Ga	23.39	46.22	ND	16.00	20.00	18.58	14.10	33.45	15.67	16.00	20.26
Y	23.17	1.37	21.00	17.90	19.20	16.94	18.79	7.95	2.78	4.20	6.19
Nb	45.20	7.47	8.00	62.90	18.20	14.22	4.21	2.99	1.55	8.50	5.98
Ta	2.12	0.31	ND	5.10	2.00	1.00	0.23	0.11	0.11	0.80	0.23
Zr	28.83	227.0	123.0	121.0	26.00	21.20	46.12	26.06	62.90	146.0	64.69
Hf	0.96	4.13	ND	1.90	0.80	0.75	1.32	0.52	1.39	2.60	1.90
Mo	3.56	0.17	ND	0.00	0.00	13.18	0.60	0.10	0.07	0.00	0.08
Sn	3.18	1.95	ND	3.30	2.90	2.48	0.54	2.37	0.66	1.80	1.42
Tl	0.75	0.21	ND	0.80	0.40	0.40	0.42	2.61	9.21	9.60	1.18
Pb	13.71	3.45	ND	11.60	11.10	12.41	9.17	9.00	21.62	19.50	28.38
U	2.21	1.74	ND	1.80	0.90	2.03	1.73	0.83	0.78	2.00	1.52
Th	11.35	0.42	ND	15.20	3.00	6.59	4.75	1.12	6.80	9.00	25.50
La	108.5	0.68	21.00	59.40	16.50	18.98	19.54	5.23	9.84	27.70	52.36
Ce	231.7	1.65	ND	140.90	34.30	39.09	41.16	13.36	22.22	48.80	88.00
Pr	21.65	0.29	ND	17.20	4.10	4.56	5.23	1.90	2.50	4.90	11.70
Nd	83.39	1.30	ND	67.70	16.30	17.05	22.06	8.75	9.34	16.40	40.32
Sm	13.45	0.35	ND	11.86	3.65	3.52	4.91	2.09	1.61	2.45	6.19
Eu	3.15	0.07	ND	2.91	1.10	1.05	0.96	0.38	0.40	0.64	0.77
Gd	8.17	0.31	ND	8.78	3.46	3.28	4.35	1.79	0.95	2.08	3.57
Tb	1.00	0.05	ND	1.04	0.59	0.53	0.62	0.24	0.11	0.22	0.41
Dy	5.25	0.31	ND	4.21	3.38	3.19	3.77	1.30	0.60	0.92	1.98
Ho	0.90	0.07	ND	0.70	0.73	0.66	0.75	0.25	0.12	0.16	0.33
Er	2.29	0.21	ND	1.72	2.07	1.98	2.14	0.73	0.40	0.48	0.79
Tm	0.28	0.04	ND	0.20	0.33	0.27	0.28	0.11	0.06	0.06	0.09
Yb	1.60	0.28	3.00	1.13	1.94	1.83	1.72	0.71	0.45	0.32	0.48
Lu	0.20	0.04	ND	0.13	0.28	0.27	0.25	0.10	0.07	0.04	0.06
W	0.55	7.81	ND	ND	ND	1.86	0.74	0.30	0.06	ND	0.09
Ge	1.15	3.24	ND	ND	ND	1.02	0.90	2.35	0.50	ND	0.89
Ag	1.30	0.26	ND	ND	ND	0.44	0.20	0.12	0.14	ND	0.20
As	1.06	0.46	ND	ND	ND	2.5	0.50	0.91	0.03	ND	0.41

Note. 1 – gneiss 73 *Hbl-Bt*, 2 – gneiss 217 *Bt* with corundum, 3 – gneiss 175/42 *Bt-Cpx*, 4 – gneiss 71 Bt, 5 – gneiss *127 Bt*, 6 – gneiss *134 Cpx-Hbl-Bt*, 7 – gneiss *128/22 Bt*, 8 – gneiss 220 *Bt-Grt*, 9 – gneiss 85a *Bt* near the contact with the Murzinka massif, 10 – 24/110 a – inclusion in the West Vatikha granite, 11 – 61 inclusion in the West Vatikha granite. 2, 8, 9 – presumably paragneisses, the remaining analyses represent orthogneisses. The number of the borehole given in the numerator, with its depth being stated in the denominator. Trace elements were determined in sample 3 at the laboratory of the Institute of Geology and Geochemistry using the emission spectral method; ND – not detectable.

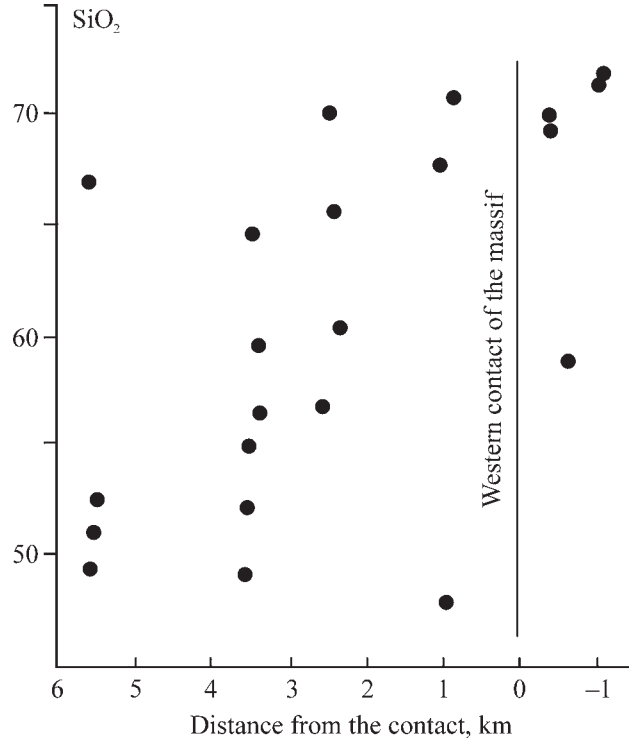

Fig. 2. Dependence of SiO_2 content in gneisses on their distance from the granite massif.

et al., 2005]. The morphological features of zircons indicate their primary crystallisation in the context of a granulite facies and subsequent diaphthorite transformations, which are about 380 million years old.

Chamber pegmatites of the gemstone belt at the base of the granite massif

Among the above-described Mesoproterozoic gneisses at the base of large granite massifs – Murzinska and Aduy – there is a Ural gemstone belt, world-famous for its chamber pegmatites characterised by rich mineralisation [Fersman, 1940]. The main features of pegmatites we will consider using the example of the Mokrusha vein, which is the most famous in the Alabashka pegmatite field (see Fig. 1) and typical of the pegmatites of the entire belt.

The vein occurs among diorite gneisses and carbonate rocks transformed into calciphyres. The host rocks have a submeridional strike and dip east at an angle of 15–20°. The vein occurs along the strike of the host rocks and transects them down the dip. The thickness of the vein ranges from 1.5–2.0 to 9–12 m. As noted above, no noticeable exocontact changes in host gneisses and carbonate rocks are observed. The veins of chamber pegmatites exhibit this feature, which distinguishes them from all other pegmatites associated with the granites of the Murzinka massif and is apparently explained by the fact that most of

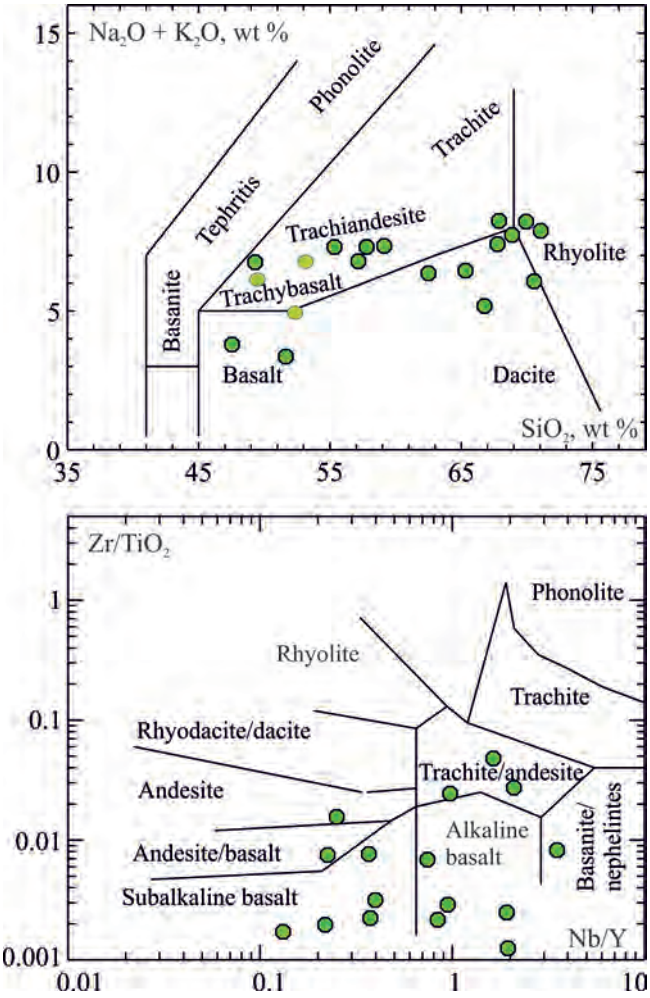

Fig. 3. Position of gneisses in classification diagrams (with authors' simplifications) [Le Maitre, 1989 (Fig. B.14); Winchester, Floyd, 1977 (Fig. 6)].

the fluid in such pegmatites is stored in vugs (cavities) inside the vein and does not interact with host rocks.

A typical cross section of a vein is given using the data of borehole 99 and is as follows. While the biotite granite of the Yuzhakovo complex (Table 2, an. 1) occurs in the hanging wall, the footwall comprises biotite diorite gneiss, which is close in composition to gneiss 128/22 (see Table 1, an. 7). The vein has cross-cutting contacts with both rock varieties. The cross section of the vein section is as follows: 23.7–24.0 m – coarse-graphic pegmatite, 24.0–25.1 m – micro-graphic pegmatite, 25.1–25.8 m – fine-graphic pegmatite, 25.8–27.0 m – block pegmatite, 27.0–29.7 m – spherulitic pegmatite, 29.7–33.2 m – fine-grained pegmatite. The compositions are given in Table 2. Fine-graphic zones (1–2 cm thick) are observed in the upper and lower endocontacts. In these zones, quartz ichthyoglipts are oriented perpendicular to the contact, which is possibly a consequence of quenching.

Table 2. Content of petrogenic (wt %) and trace (ppm) elements in granite from the hanging wall of the Mokrusha pegmatite vein (1) and from graphic pegmatites of this vein (2–5). Borehole 99

Element	1	2	3	4	5	6	Element	1	2	3	4	5	6
SiO_2	72.11	74.84	75.2	77.02	76.19	74.92	Zr	54.58	11.95	11.03	13.44	40.00	46.29
TiO_2	0.18	0.05	0.02	0.01	0.01	0.03	Hf	1.13	0.65	1.02	0.92	5.08	2.75
Al_2O_3	14.64	12.99	12.71	12.63	13.18	12.74	Mo	0.57	0.04	0.22	0.16	0.39	0.15
Fe_2O_3	0.38	0.33	0.19	0.11	0.96	0.35	Sn	0.54	0.69	8.92	9.24	15.46	2.20
FeO	1.49	1.87	1.74	1.95	1.92	1.72	Tl	0.41	0.65	1.99	1.70	1.36	1.68
MnO	0.06	0.02	0.03	0.05	0.55	0.04	Pb	15.77	34.79	29.87	26.78	7.34	24.81
MgO	0.28	0.1	0.1	0.1	0.1	0.1	U	59.73	1.56	2.33	1.99	18.12	11.23
CaO	1.21	1.17	0.91	0.58	0.44	0.61	Th	4.99	11.60	2.66	0.96	8.08	22.63
Na_2O	3.35	4.11	3.89	5	4.77	4.02	La	33.18	3.93	2.31	1.84	6.50	4.47
K_2O	5.78	4	5.05	2.18	1.14	4.88	Ce	54.13	9.06	5.02	3.94	18.13	11.94
P_2O_5	0.08	0.01	0.01	0.01	0.01	0.01	Pr	5.53	1.21	0.54	0.39	2.39	1.67
Impurities	0.39	0.05	0.1	0.21	0.69	0.3	Nd	18.25	4.81	1.80	1.27	9.01	6.84
Σ	99.95	99.57	99.95	99.85	99.96	99.72	Sm	2.34	1.15	0.65	0.40	5.70	2.17
Li	57.31	50.35	405.50	496.86	352.86	12.91	Eu	1.20	0.06	0.01	0.00	0.02	0.06
Rb	60.98	81.23	253.63	348.64	290.42	174.60	Gd	1.31	0.85	0.65	0.45	11.88	1.98
Cs	6.54	5.44	74.95	69.29	52.29	7.85	Tb	0.14	0.11	0.13	0.09	3.47	0.32
Be	2.28	1.57	4.16	4.87	15.70	4.86	Dy	0.72	0.51	0.85	0.55	24.59	1.93
Sr	353.73	10.96	1.11	0.90	2.83	7.56	Ho	0.12	0.08	0.15	0.10	4.24	0.43
Ba	970.37	19.97	8.05	6.82	14.73	8.87	Er	0.30	0.19	0.43	0.28	10.32	1.43
Sc	3.13	1.53	5.63	7.58	17.15	3.74	Tm	0.04	0.02	0.06	0.04	1.34	0.23
V	20.19	1.32	0.33	0.48	0.45	0.44	Yb	0.22	0.15	0.41	0.26	7.48	1.68
Cr	1.01	0.66	1.71	2.28	0.63	1.45	Lu	0.03	0.02	0.05	0.03	0.76	0.27
Co	3.03	0.25	0.07	0.11	0.10	0.15	W	8.70	0.66	2.42	2.24	12.20	0.85
Ni	1.64	0.72	0.31	0.48	0.39	1.45	Bi	0.03	0.04	4.88	3.47	6.35	0.47
Cu	9.95	2.67	2.58	6.47	3.04	3.24	Cd	0.04	0.03	0.08	0.08	0.32	0.06
Zn	49.43	11.15	47.56	63.29	63.00	12.01	Ge	0.71	1.25	2.38	3.08	3.59	1.71
Ga	21.05	16.23	21.31	27.79	30.20	16.07	Ag	0.54	0.24	0.85	0.71	1.18	0.42
Y	3.68	1.57	3.79	3.65	157.88	7.32	Sb	0.36	0.41	0.72	0.71	2.20	0.20
Nb	18.23	7.41	29.51	34.01	40.42	13.04	As	1.27	1.40	5.34	6.05	8.22	0.47
Ta	0.30	0.42	2.74	2.39	4.93	1.70							

Note. 1 – a depth of 23.4 m (granite in contact with the vein); 2–5 – graphic texture: 2 – 23.7 m, 3 – 24.3 m, 4 – 25.1 m, 5 – 43.0 m – fine graphic texture in the upper endocontact of the vein.

The widespread development of graphic intergrowths of quartz with plagioclase and potassium feldspar provided the possibility to study the conditions for the formation of pegmatites of the Mokrusha vein in detail. These structures always arise as a result of eutectic crystallisation under conditions close to the system $P_{H_2O} = P_{total}$. The content of quartz in such intergrowths is strictly correlated with the composition of feldspar and is determined by the pressure during crystallisation [Fershtater, 1987]. The results of studying the cross section of the vein (borehole 99) in terms of the composition of quartz-feldspar intergrowths are given in Table 3.

The obtained data indicate meso-abyssal conditions for the formation of the Mokrusha vein. An increase in the quartz content in quartz-feldspar intergrowths in the granite of the hanging wall, which is in direct contact with the vein, and in the zone of fine-grained pegmatite at the base of the vein (and, accordingly, lower pressure values) is apparently due to a decrease in P_{H_2O}. All other pressure values correspond to $P_{H_2O} = P_{total}$.

Table 3. Quartz content in graphic intergrowths with K-feldspar and plagioclase in the croee section of the Mokrusha vein, borehole 99 (according to the results of counting in thin sections)

Zone	Depth, m	Quartz content, vol %		P_{H_2O}, kb
		Fsp + Q	*Pl + Q*	
Host adamellite	23.3–23.7	39	44	2
Coarse-graphic	23.7–24.0	33	40	3
Micro-graphic	24.0–25.1	34	38	3–4
Micro-graphic	25.1–25.8	33	38	3–4
Block	25.8–27.0	–	–	–
Spherulitic	27.0–29.7	33	37	3–4
Fine-grained pegmatite	29.7–33.2	38	41	2

It is important to note that chamber pegmatites of the Mokrusha type exhibit a particular geochemical feature, which reliably distinguishes them from all other pegmatites associated with various granites of the Mur-

zinska massif. Mokrusha pegmatites (see Table 2) are characterised by an extremely low (less than 10 ppm) content of Sr and Ba with low K/Rb (<100) and Zr/Hf (<20) ratios, whereas in all other pegmatites the abovementioned parameters are similar to those of granites. These features indicate that Mokrusha pegmatite bodies did not participate in the formation of granite massifs. At the same time, such pegmatites in many cases complete the evolutionary trends of granites of the Murzinska massif, which allows us to consider them as the latest manifestations of granite magmatism, which is consistent with the K-Ar age of pegmatite mica coming to 220–250 Ma [Borshchov, Fershtater, 2017]. The presented data suggest that most of chamber pegmatites of the gemstone belt formed after the completion of granite magmatism, which formed the Murzinka massif. It can be assumed that the granite component of chamber pegmatites is not manifested. An example would be the pegmatite fields in Norway and Sweden consisting of many thousands of pegmatite veins that show no connection with granites [Muller et al., 2017].

Yuzhakovo complex of veined granitoids

The granitoids of this complex are localised west of the Murzinska massif, within the metamorphic complex. They do not form large bodies; however, the numerous veins of these rocks often predominate in volume over the host metamorphic rocks.

Early veins (first generation) are represented by biotite gneiss-like plagiogranites, usually in the form of ptygmatic folds (Table 4, an. 1–3, 5). The rocks comprise antiperthite plagioclase An_{30-40}, quartz and red-brown high-titanium biotite. Rare potassium feldspar is represented by orthoclase, with the accessory minerals including apatite and sphene. The plagiogranite formation is completed by thin plagiopegmatite veins and plagiogranite areas, followed by gneiss-like or massive granites and adamellites characterised by a higher potassium content, which varies widely, reaching 4.78 wt % (see Table 4, an. 4, 6). It should be noted that the gneissic structure of such veins always coincides with their strike, i.e. it is, clearly, syngenetic and, naturally, has a different direction as compared to earlier plagiogranites.

Second-generation veins represented by granites and adamellites are most widespread (see Table 4, an. 7–11). These rocks often exhibit gneissic structures, whose direction does not coincide with that of the gneissic structures in the first-generation veins. Similar associations are repeated in all outcrops and indicate that the granites of the Yuzhakovo complex formed under orogenic conditions: each completed episode of granite formation, whose completion is indicated by the presence of pegmatites, corresponded to its own stress direction. The episodes of tectonic and magmatic activity coincided. It should be noted that all the veins of the Yuzhakovo complex constitute intrusive bodies, which are not associated with any noticeable migmatisation (partial melting). The development of insignificant quartz-feldspar areas in gneisses, possibly associated with partial melting, precedes the introduction of the earliest veins of the Yuzhakovo granites.

Murzinka Massif

Western part – Vatikha complex. The identification of granites making up the western part of the Murzinka massif as a separate complex was determined by the distinctive petrographic character of rocks including antiperthite plagioclase An_{20-25} and poorly structured feldspath (orthoclase) [Orogenic granitoid magmatism..., 1994]. These mineralogical features bring Vatikha granites closer to the Yuzhakovo ones; however, unlike the latter, the Vatikha granites form a large body, constituting at least half of the total volume of the Murzinka Massif, rather than separate veins. The rocks are characterised by a prismatic-granular structure and contain porphyritic segregations of orthoclase and magnetite. The presence of the latter is due to the increased magnetic field in the western part of the massif, which clearly marks the distribution of Vatikha rocks. The plagioclase present in them is noticeably enriched with the albite component as compared to plagioclase in the Yuzhakovo granites of the same silica content (60–70 and 75–80 mol %, respectively). Accessory minerals are diverse – orthite, apatite, zircon, xenotime and monazite.

In the western part of the complex, the predominating adamellites and granites contain the xenoliths of more melanocratic rocks of granodiorite and adamellite composition, which we interpret as protolith restites preserved under a high degree of the partial melting of rocks having a composition close to that of adamellite (see Table 1, an. 9–11). The granites and adamellites that formed have a specific composition (Table 5, an. 1–4) and are identified as the West Vatikha subcomplex. It is these granites that exhibit the strongest similarities with the Yuzhakovo granites. Granites occurring to the east of the East Vatikha subcomplex are much more uniform in composition (see Table 5, an. 5–7) than the West Vatikha granites; they do not contain antiperthite plagioclase and are slightly enriched with rubidium, as compared to the latter, in accordance with the general geochemical zonation of the massif (see below).

Eastern part of the Murzinka massif – Murzinka complex. These granites intrude the Vatikha granites in the west, as well as volcanic-sedimentary and sedimentary rocks metamorphosed in the context of greenschist and epidote-amphibolite facies in the east. Near the top, granites become leucocratic; the number of aplite and pegmatite veins in them increases, reaching 50–60% of the volume. The contact itself is typically of the injection type: numerous granite apophyses, aplite and pegmatite veins penetrate the host rocks, which un-

Table 4. Content of petrogenic (wt %) and trace (ppm) elements in the granites of the Yuzhakovo complex

No.	1	2	3	4	5	6	7	8	9	10	11
Sample	112a	128	114	112b	129	115_2	130	131	123	128/52	84b
SiO_2	73.99	72.5	69.81	72.28	72.1	70.21	71.68	70.76	68.9	70.02	71.22
TiO_2	0.08	0.10.	0.19	0.06	0.14	0.26	0.13	0.25	0.39	0.670	0.17
Al_2O_3	15.45	15.9	15.65	14.09	15.8	15.09	15.47	15.29	15.9	13.39	15.38
Fe_2O_3	0.45	ND	1.12	0.53	ND	0.3	0.1	0.39	0.24	2.05	0.26
FeO	0.8	1.37	2.55	3.98	1.69	2.01	1.48	1.61	2.24	2.1	2.61
MnO	0.05	ND	0.05	0.05	0.01	0.05	0.05	0.05	0.05	0.020	0.05
MgO	0.26	0.31	0.61	0.24	0.43	0.59	0.27	0.43	0.56	1.39	0.35
CaO	2.67	2.95	4.19	1.87	3	1.46	2.11	1.31	1.33	1.68	1.66
Na_2O	4.56	4.82	3.69	4.03	4.61	3.79	4.25	3.94	3.4	3.17	3.12
K_2O	0.67	0.81	0.69	2.2	0.86	4.78	3.15	4.61	5.68	4.99	4.6
P_2O_5	0.05	0.05	0.12	0.05	0.05	0.09	0.11	0.08	0.11	0.131	0.05
Impurities	0.16	0.32	0.65	0.43	0.44	0.33	0.11	0.12	0.24	0.3	0.44
Σ	99.19	99.12	99.37	99.81	98.14	96.7	100.28	100.16	99.04	99.89	99.91
Li	43.45	9	13	31.63	15	38.57	11	15	32.34	9.87	10.07
Rb	2.62	7	14	26.27	25	56.75	40	95	57.76	83.41	48.55
Cs	0.42	0.5	0	0.25	0.8	0.91	1	1	1.71	0.55	0.47
Be	9.59	1.9	1	5.24	1.5	3.53	3	1	2.88	1.35	0.88
Sr	177.9	286	533	283.7	441	298.5	365	521	231.7	413.1	803.2
Ba	104.4	135	78	349.8	238	1143	960	0	1612	1303	1877
Sc	15.89	1.3	10	6.5	21.1	8.97	4	8	5.42	5.03	1.14
V	18.48	12	20	18.38	18	35.31	9	17	46.33	47.90	9
Cr	22.3	0	0	27.44	0	14.72	0	2	15.38	4.95	3.83
Co	3.44	1.3	2	4.09	2.2	4.47	1	3	4.99	4.90	1.4
Ni	32.74	0	0	24.39	0	10.64	0	4	5.25	2.89	3.19
Cu	12.6	0	1	50.38	0	11.5	3	11	11.07	9.70	10.13
Zn	33.85	11	27	42.14	19	95.55	0	33	106.1	66.58	49.59
Ga	39.89	17	16	28.51	15	27.5	12	9	33.46	20.16	15.06
Y	1.61	1	8	0.72	3.7	1.44	5.2	3.2	1.52	3.61	2.17
Nb	4.65	1.3	4.3	1.38	2.3	6.07	4.3	3.3	9.62	7.89	0.87
Ta	0.18	0.1	1.9	0.07	0.2	0.17	0.7	0.3	0.32	0.28	0.07
Zr	47.21	54	14	24.03	121	230.5	143	213	359.5	55.28	83.77
Hf	1.41	1.7	0.3	0.6	3.2	3.51	3	3.9	5.87	1.35	2.15
Mo	2.94	ND	0	1.69	ND	0.65	0	0	0.42	1.41	0.05
Sn	1.61	ND	0.2	1.98	ND	3.31	1.6	1.4	2.2	1.18	0.53
Tl	0.15	ND	0.2	0.2	ND	0.5	0.4	0.5	0.58	0.40	0.66
Pb	15.47	13	6.6	19.14	14	30.61	24.1	33.8	28.63	16.35	22.09
U	0.39	0.5	0.2	0.44	1.9	1.91	0.6	1.7	2.46	1.02	1.23
Th	1.98	3.5	0.5	1.95	11	5.91	6	14.6	10.1	24.74	7.53
La	0.58	3.5	5.4	1.25	15	5.54	12.5	41.7	15.2	101.6	7.61
Ce	1.69	12	16.7	2.48	39	11.94	45.2	70.9	29.79	184.7	16.36
Pr	0.22	0.78	1.5	0.37	3.1	1.36	3.2	7.5	3.05	14.71	1.93
Nd	0.95	2.5	6.1	1.4	11	4.9	11.9	24.7	9.95	46.62	7.4
Sm	0.32	0.6	1.35	0.34	1.8	0.84	2.65	3.36	1.33	5.23	1.38
Eu	0.19	0.53	0.68	0.23	0.85	0.2	1.17	1.11	0.25	1.32	0.48
Gd	0.34	0.4	1.37	0.23	1.3	0.55	2.26	2.44	0.57	2.29	0.86
Tb	0.05	0.05	0.22	0.03	0.15	0.07	0.27	0.22	0.06	0.22	0.1
Dy	0.29	0.26	1.31	0.17	0.72	0.32	1.19	0.79	0.29	0.94	0.52
Ho	0.05	0.03	0.29	0.03	0.15	0.06	0.2	0.12	0.05	0.14	0.09
Er	0.15	0.07	0.86	0.08	0.37	0.14	0.54	0.35	0.14	0.35	0.26
Tm	0.02	0.01	0.14	0.01	0.06	0.02	0.07	0.04	0.02	0.04	0.04
Yb	0.14	0.03	0.89	0.08	0.35	0.12	0.44	0.21	0.15	0.24	0.22
Lu	0.02		0.14	0.01	0.06	0.02	0.06	0.03	0.02	0.03	0.04

Note. 1-6 – the first generation of veins, 7-11 – the second generation of veins, ND – not detectable.

Table 5. Content of petrogenic (wt %) and trace (ppm) elements in the granites of the Vatikha (1–7) and Murzinka (8–12) complexes

No.	1	2	3	4	5	6	7	8	9	10	11	12
Sample	91	92	66	57	106	15	10	17	23	26	42	51
SiO_2	72.56	71.12	72.48	71.03	73.16	72.88	71.19	74.66	73.87	74.15	72.48	72.65
TiO_2	0.15	0.13	0.14	0.17	0.17	0.12	0.24	0.47	0.09	0.10	0.14	0.11
Al_2O_3	14.80	14.25	14.88	14.59	14.30	12.99	14.69	13.83	13.65	14.23	15.27	14.74
Fe_2O_3	0.10	0.31	0.49	0.55	0.31	0.45	0.42	0.10	0.34	0.23	0.10	0.45
FeO	1.67	2.51	1.22	2.12	2.04	1.74	2.60	1.61	2.06	2.14	1.58	1.35
MnO	0.05	0.05	0.05	0.05	0.05	0.05	0.05	0.05	0.05	0.05	0.05	0.05
MgO	0.37	0.31	1.40	0.36	0.93	0.98	0.35	0.11	0.29	0.14	0.29	0.24
CaO	1.18	1.35	1.40	1.07	0.93	0.98	1.19	0.96	0.64	0.80	1.48	1.18
Na_2O	3.64	3.85	3.88	3.45	3.62	3.79	3.39	3.70	3.51	3.64	4.82	4.50
K_2O	5.34	4.68	4.33	5.05	5.15	4.23	4.31	4.50	4.50	4.54	3.19	3.34
P_2O_5	0.08	0.09	0.05	0.08	0.05	0.05	0.07	0.05	0.05	0.05	0.05	0.05
Σ	99.96	98.65	98.24	99.03	98.63	99.33	98.80	99.14	99.05	98.66	99.45	98.66
Li	10.12	11.35	7.00	10.70	9.00	13.00	16.00	17.00	24.00	36.00	100.00	135.00
Rb	61.89	66.71	71.00	86.19	137.0	124.0	131.0	176.0	257.0	266.0	105.0	129.0
Cs	0.37	0.51	0.00	0.63	1.00	1.00	1.00	1.00	1.00	2.00	5.00	8.00
Be	1.71	1.95	2.00	1.22	1.00	2.00	1.00	2.00	2.00	3.00	3.00	6.00
Sr	216.3	212.8	313.0	212.2	142.0	89.0	259.0	107.0	96.0	106.0	200.0	336.0
Ba	1048	895.5	779.0	982.8	482.0	282.0	0.0	318.0	355.0	343.0	721.0	0.0
Sc	1.51	2.89	6.00	3.11	6.00	7.00	8.00	8.00	10.00	8.00	6.00	5.00
V	8.60	14.86	10.00	19.22	4.00	6.00	15.00	4.00	2.00	5.00	14.00	13.00
Cr	1.76	5.95	0.00	37.89	0.00	0.00	0.00	0.00	0.00	0.00	0.00	0.00
Co	1.02	1.90	1.00	2.61	1.00	1.00	2.00	1.00	1.00	1.00	1.00	1.00
Ni	1.20	5.43	0.00	57.45	0.00	0.00	0.00	0.00	0.00	0.00	0.00	0.00
Cu	3.73	11.73	9.00	13.82	1.00	1.00	5.00	1.00	1.00	1.00	7.00	1.00
Zn	33.59	38.17	0.00	47.01	0.00	13.00	28.00	31.00	38.00	26.00	24.00	24.00
Ga	16.68	18.18	14.00	19.59	15.00	18.00	12.00	19.00	21.00	20.00	17.00	10.00
Y	1.69	2.01	2.60	2.39	9.40	6.80	6.90	6.50	12.10	6.90	1.90	2.10
Nb	2.61	4.00	2.80	5.69	11.50	11.10	15.40	14.60	23.30	19.40	14.40	10.20
Ta	0.14	0.27	0.20	0.25	2.20	1.30	1.60	1.20	23.40	2.20	1.50	2.20
Zr	83.13	40.95	149.00	84.88	145.0	93.00	204.0	93.00	103.0	106.0	125.0	106.0
Hf	2.74	1.44	3.10	2.38	3.50	2.60	4.40	2.70	2.90	2.80	3.10	2.50
Mo	0.06	0.39	0.30	8.33	0.00	0.00	0.00	0.00	0.00	0.00	0.00	0.00
Sn	0.78	1.34	0.30	1.73	0.70	1.50	0.70	2.10	5.10	3.00	3.40	4.40
Tl	0.87	0.58	1.90	0.70	1.00	6.80	0.80	1.20	1.30	2.80	4.00	1.10
Pb	30.99	26.54	18.00	31.44	25.50	25.20	28.10	33.40	33.90	27.60	19.90	19.90
U	0.77	0.79	0.70	1.47	2.60	2.20	3.10	2.70	5.50	2.90	1.50	1.30
Th	17.26	26.21	31.40	16.97	37.40	22.00	22.90	22.10	29.20	25.30	3.70	2.20
La	14.48	27.25	14.30	30.68	76.50	38.20	63.50	41.30	44.50	45.10	7.60	5.50
Ce	36.68	42.10	39.80	63.18	140.20	73.20	117.70	77.30	83.60	84.50	14.00	10.70
Pr	3.66	4.72	3.00	7.21	14.70	7.90	11.80	8.30	8.90	9.00	1.60	1.20
Nd	12.54	16.22	10.60	24.15	48.50	25.90	37.40	27.10	29.00	29.40	5.40	4.20
Sm	2.11	2.61	1.98	3.68	8.35	5.02	5.22	5.47	5.93	5.14	0.96	0.80
Eu	0.49	0.52	0.68	0.58	0.67	0.47	0.97	0.57	0.57	0.53	0.29	0.33
Gd	1.09	1.57	1.57	2.01	6.51	3.91	4.06	4.23	4.85	3.98	0.77	0.63
Tb	0.13	0.15	0.17	0.19	0.75	0.48	0.43	0.48	0.65	0.46	0.09	0.09
Dy	0.67	0.73	0.68	0.84	2.63	1.89	1.67	1.79	2.69	1.81	0.37	0.43
Ho	0.11	0.12	0.11	0.13	0.39	0.28	0.29	0.26	0.47	0.28	0.06	0.06
Er	0.30	0.28	0.24	0.33	0.91	0.61	0.81	0.60	1.11	0.67	0.16	0.16
Tm	0.04	0.03	0.03	0.04	0.08	0.07	0.11	0.06	0.16	0.08	0.02	0.03
Yb	0.22	0.20	0.17	0.22	0.44	0.41	0.72	0.37	0.87	0.52	0.14	0.14
Lu	0.03	0.03	0.01	0.03	0.05	0.05	0.11	0.05	0.12	0.07	0.02	0.02

Note. The Vatikha complex: west (1–4) and east (5–7) subcomplexes, the Murzinka complex (8-12): numbers of samples increase from west to east.

dergo strong hydrothermal transformations – micasisation, silicification, albitisation, and K-feldsparisation.

The compositions of granites are given in Table 5 (an. 8–12). These are predominantly two-mica varieties. Biotite predominates in the western part, with the role of muscovite growing in the eastern part. Spessartine-almandine garnet, which is more common for aplites and pegmatites, often occurs in paragenesis with muscovite. Plagioclase is characterised by an even higher content of the albite component than in Vatikha granites – An_{12-18}. Antiperthites are absent. Potassium feldspar is represented by both orthoclase and microcline. The role of the latter is growing from west to east. Myrmekite is widespread.

ISOTOPIC STUDIES

Isotopic studies reveal that the granitoids of the Vatikha and Murzinka complexes exhibit approximate uniformity in terms of ages. The ^{207}Pb-^{206}Pb age of zircon and the Rb-Sr age of the rock are generally the same – 254 ± 5 Ma [Montero et al., 2000; Gerdes et al., 2002], whereas the values of $^{87}Sr/^{86}Sr$ and εNd_{255} (Table 6) indicate a different substrate.

Yuzhakovo plagiogranites are characterised by a low initial $^{87}Sr/^{86}Sr$ ratio and a positive or near-zero εNd value, while the eastern granites of the Yuzhakovo complex located near the Murzinka massif (sample 115) and Vatikha granites have high $^{87}Sr/^{86}Sr$ ratios and negative εNd_{255} values (Sr_i = 0.70868–0.70923 and εNd_{255} from –8.9 to –11.9), indicating their origin from an ancient sialic substrate. Murzinka granites are markedly different in their geochemical parameters. They are characterised by the low contents of radiogenic Sr (Sr_i = 0.70419–0.70549) and the near-zero values of εNd_{255} (from –2.6 to +2.3), which fall to –8.9 only in the westernmost part of the complex (see Table 6, sample 22). There is practically no doubt that the rocks of the newly formed crust – possibly similar to the Silurian-Devonian volcanic-sedimentary strata that are in contact with Murzinka granites – constituted the substrate of these granites.

Geochemical zonation

The identified granite complexes are markedly different in their geochemical parameters. In terms of most petrogenic elements, the granitoids of different complexes exhibit uniformity, except for the early granites of the Yuzhakovo complex characterised by high calcium and low potassium contents (Fig. 4). The most striking differences are detected in the concentrations of rubidium, according to which granites form a clear evolutionary series (in increasing order of element concentrations): 1) first-generation veins of the Yuzhakovo complex; 2) second generation veins of the Yuzhakovo complex, West Vatikha subcomplex; 3) East Vatikha subcomplex; 4) Murzinka complex. A similar trend is observed for niobium and tantalum. The K/Rb, Zr/Hf and Nb/Ta ratios, as well as barium and strontium contents, decrease in the same direction (Fig. 5). Importantly, the same trend is clearly observed for lithium, whose contents increase sharply in the granites of the Murzinka complex (Fig. 6).

The spatial distribution of the described trends is demonstrated by the geochemical profile of the Murzinka massif (Fig. 7). It is easy to see that within the massif, i.e. in the rocks of the Vatikha and Murzinka complexes, Rb and Li contents gradually increase from west to east and the K/Rb ratio decreases. In terms of potassium content and the K/Rb ratio, the rocks of the Yuzhakovo complex do not exhibit this trend. However, in terms of the K/Rb ratio, the rocks of second-generation veins follow the general trend.

The geochemical zonanation of the rocks is naturally reflected in the composition of such rock-forming minerals as plagioclase and biotite. As previously noted, the content of the anorthite component in plagioclase naturally decreases from the Yuzhakovo complex to the Murzinka complex, with the titanium content decreasing and the contents of rubidium and lithium increasing in biotite in the same direction (Fig. 8). Recent data indicate that the described geochemical zonation emerged at the magmatic stage, given that the above-mentioned minerals characterise

Table 6. Sr and Nd isotopic parameters of the rock as a whole for the granites of Yuzhakovo (1–3), Vatikha (4–6) and Murzinka (7–10) complexes according to [Gerdes et al., 2002]

No.	Sample	Rb	Sr	$^{87}Rb/^{86}Sr$	$^{87}Sr/86^{Sr}$	$^{87}Sr/^{86}Sr_i$	Sm	Nd	$^{147}Sm/^{144}Nd$	$^{143}Nd/^{144}Nd$	εNd_{255}	D, km
1	129	26.5	519	0.1476	0.7047	0.70416	1.8	10.63	0.1026	0.512692	4.1	ND
2	128	77.8	393	0.572	0.70629	0.70418	ND	ND	ND	ND	ND	ND
3	115	124	409	0.8803	0.71241	0.70922	2.8	17.69	0.0956	0.512467	–0.05	ND
4	61	60.6	181	0.9711	0.71275	0.70923	3.02	19.45	0.0938	0.51196	–9.9	1.5
5	9	139	130	2.687	0.71886	0.70912	3.34	21.39	0.0945	0.511942	–10.3	4.7
6	17	164	96	4.948	0.72663	0.70868	3.38	16.11	0.1269	0.511911	–11.9	4.8
7	22	214	73	8.523	0.7354	0.70447	3.07	15.89	0.1169	0.512048	–8.9	6.0
8	42	168	250	1.949	0.71166	0.70459	0.92	4.89	0.1142	0.512659	2.3	8.0
9	50	210	106	5.725	0.72496	0.70419	2.87	15.92	0.1088	0.512359	–2.6	9.1
10	51	123	288	1.234	0.70997	0.70549	0.54	2.65	0.1277	0.512634	2.3	9.1

Note. D – distance from the western contact of the massif. See rocks compositions in Tables 4 and 5. ND – not detectable.

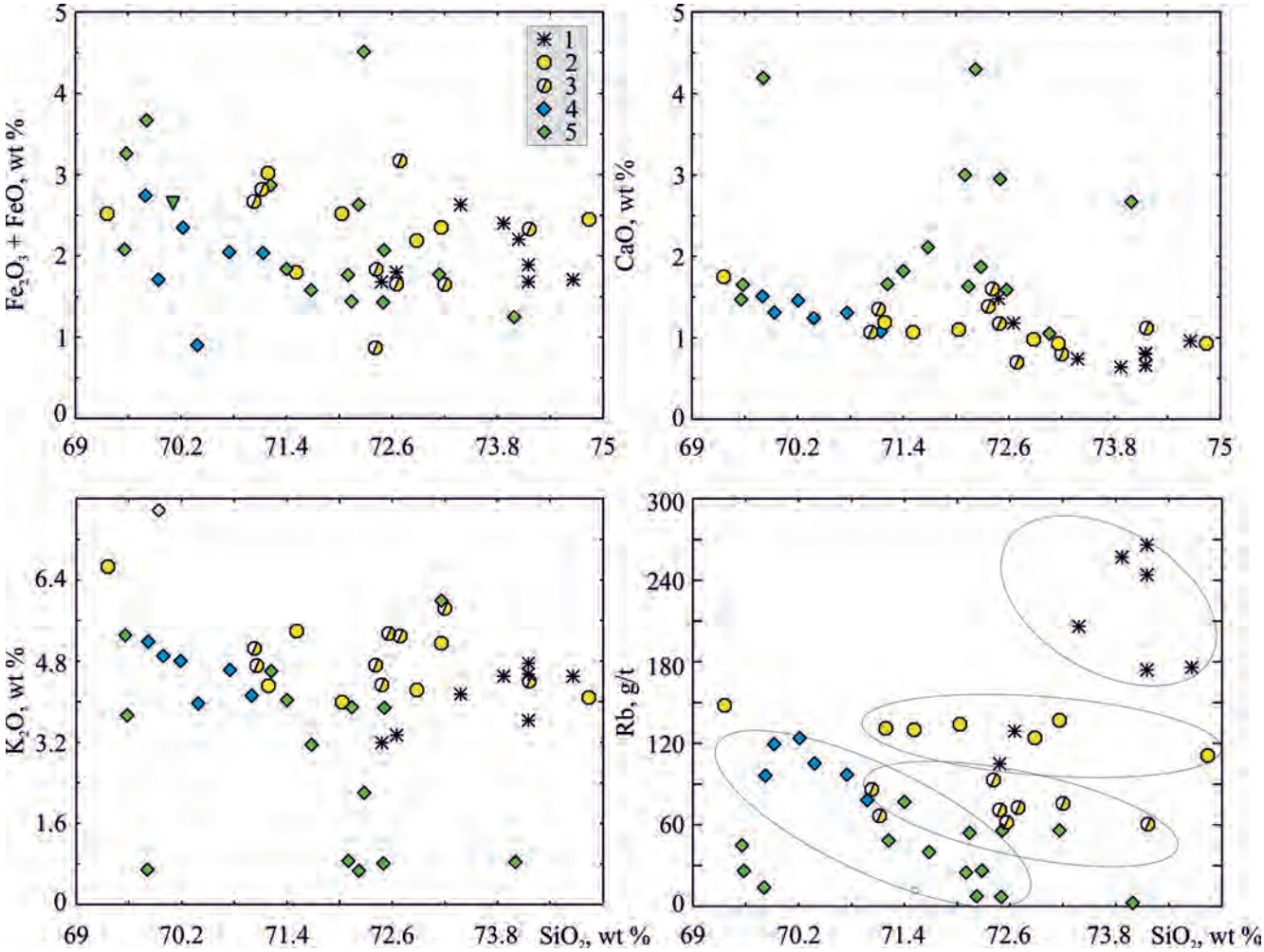

Fig. 4. (Fe_2O_3 + FeO), CaO, K_2O, Rb versus SiO_2 for granites.

Complexes: 1 – Murzinka; 2 – West Vatikha; 3 – East Vatikha; 4, 5 – Yuzhakovo: 4 – first generation of veins, 5 – second generation of veins.

precisely this stage of rock formation. As for the intense hydrothermal activity at the top of the massif, it is caused by a fluid released from the crystallising granite melt and is enriched with such elements as rubidium, lithium, niobium and tantalum, which granites are also rich in.

The clearly expressed geochemical zonation of the Murzinka Massif is accompanied by the increasing number of pegmatoid granites in the eastward direction (towards the top of the massif). They are noted throughout the entire cross section of the massif and uniformly share common geochemical features with host granites, thus being part of in the general zonation of the massif. This feature indicates that pegmatoid granites are the products of magmatic evolution that occurred there and confirms the conclusion made earlier about the magmatic nature of zonation drawing on a regular change in the composition of the main rock-forming minerals – plagioclase and biotite. It can be assumed that during the crystallisation of granite magma saturated with water, even at the magmatic stage, fluid enriched with elements (rubidium, lithium, niobium, tantalum, hafnium and beryllium) is separated and gradually concentrated in the upper part of the massif. Naturally, granites are enriched with the specified elements as well. It can be assumed that the proposed mechanism underlying the fluid-magma differentiation ensures the geochemical zonation of the massif, as well as creates a metasomatic halo and rich mineralisation (niobium, tantalum, molybdenum, beryllium, emeralds) in the zone overlying intrusions, which is most vividly manifested in association with the Aduy massif – the southern continuation of Murzinka.

A clear one-sided geochemical zonation, common for the entire massif, is consistent with its interformational position and stratiform shape, indicating the existence of a single magma chamber where the differentiation of the crystallising melt took place. This is also

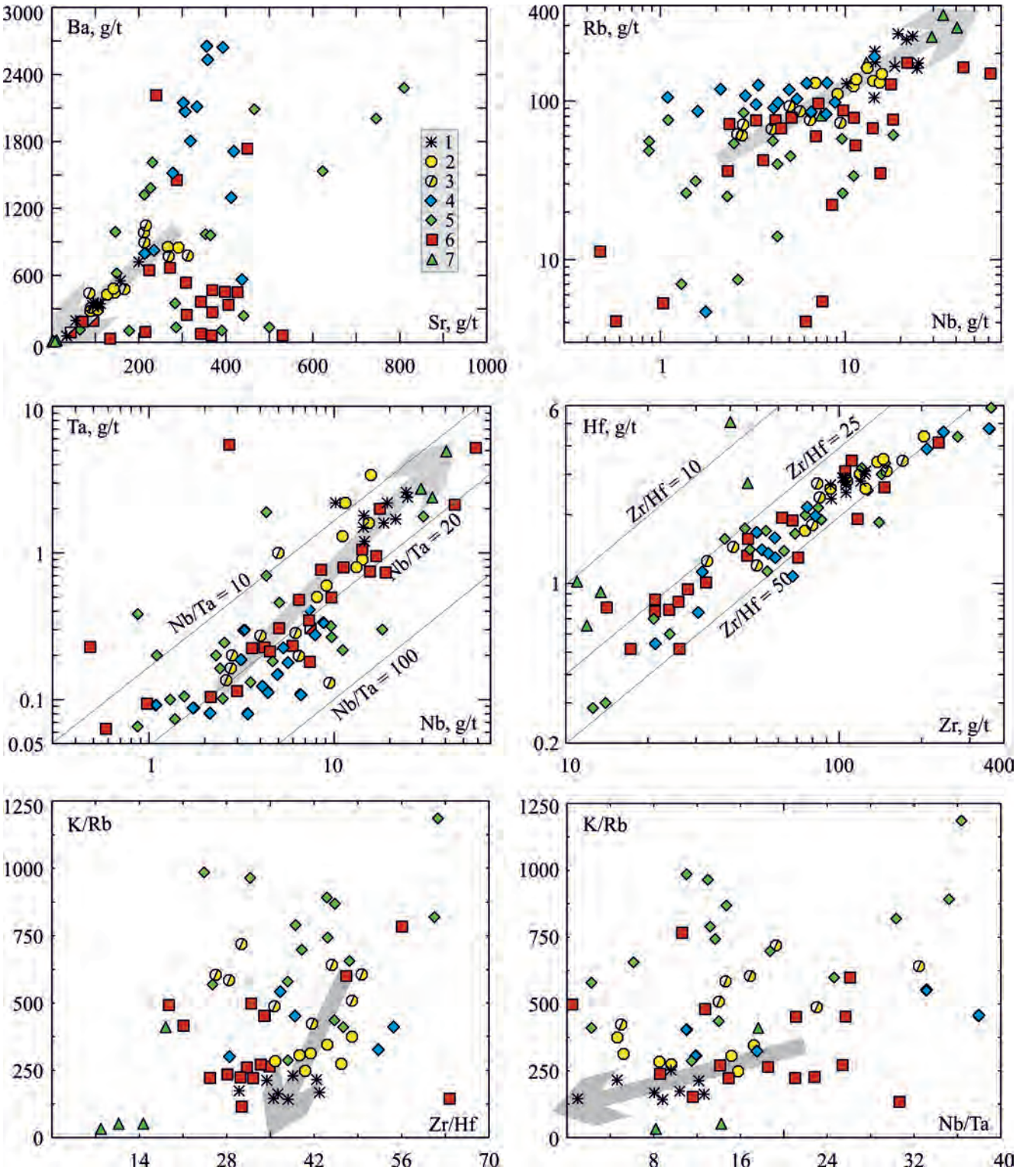

Fig. 5. Diagrams showing the distribution of trace elements in granites, pegmatites and gneisses.

1–5 – the same as in Fig. 4; 6 – gneisses, 7 – chamber pegmatites of the gemstone belt. The thick grey lines with arrows show West-East trends for the granites of the Murzinka massif.

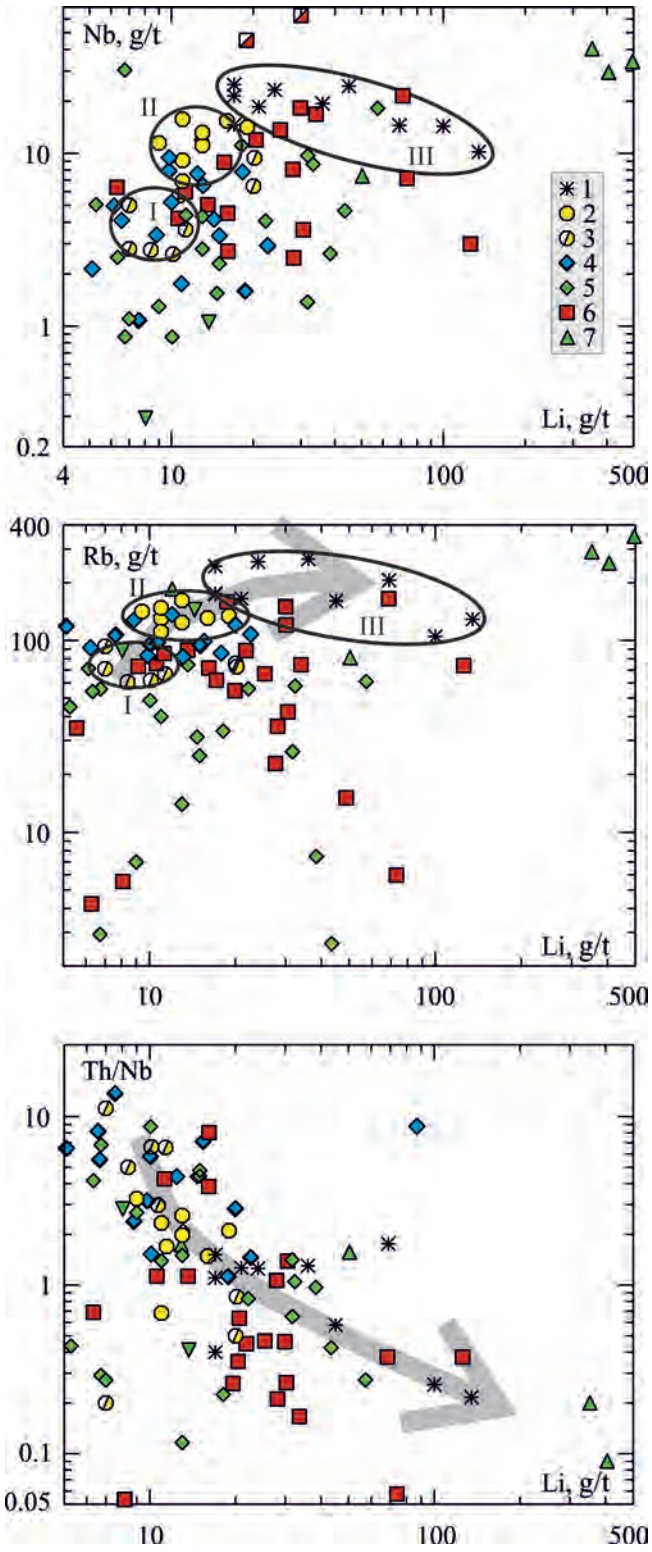

Fig. 6. Nb, Rb and Th/Nb versus Li for granites, pegmatites and gneisses.

Symbols are the same as for Fig. 5. The ovals mark the areas of the West Vatikha (I) and East Vatikha (II) subcomplexes and the Murzinka complex (III) where granites are concentrated.

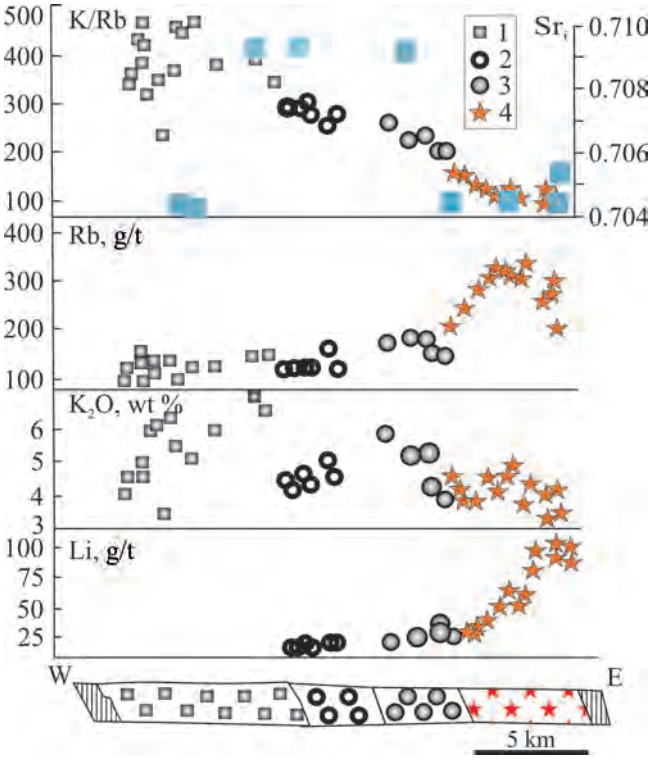

Fig. 7. Distribution of K, Rb, Li in the latitudinal section of granites.

1 – Yuzhakovo, 2 – West Vatikha, 3 – East Vatikha, 4 – Murzinka complexes. In the top diagram, blue bars indicate the values of $^{87}Sr/^{86}Sr_i$.

evidenced by the same isotopic age (Rb-Sr whole-rock and U-Pb zircon ages) of all granitoids being estimated at approximately 255 Ma. However, clear isotopic differences between the Vatikha granites of the western part of the massif and the granites of the Murzinka complex, which make up its eastern half (see Fig. 7), indicate different magmatic sources for both granites. This is also evidenced by the behaviour of potassium, which follows the usual homodromous trends within different complexes, first revealing an increase in the contents in the east for the Yuzhakovo, Vatikha and Murzinka complexes, and then a decrease in the concentration in the latter two (see Fig. 7). Unlike such elements as Rb, Li, Be, Nb and Ta, whose geochemistry is largely determined by fluid transport, the behaviour of potassium follows the laws of crystallisation differentiation. Thus, the modern appearance of the massif results from the evolution of the magmatic melt and the fluid that is in equilibrium with it.

RESULTS AND DISCUSSION

Mesoproterozoic para- and orthogneisses of various compositions, metamorphosed in the context of a granulite facies of regional metamorphism, occur in the bottom of the Murzinka massif. The coexisting horn-

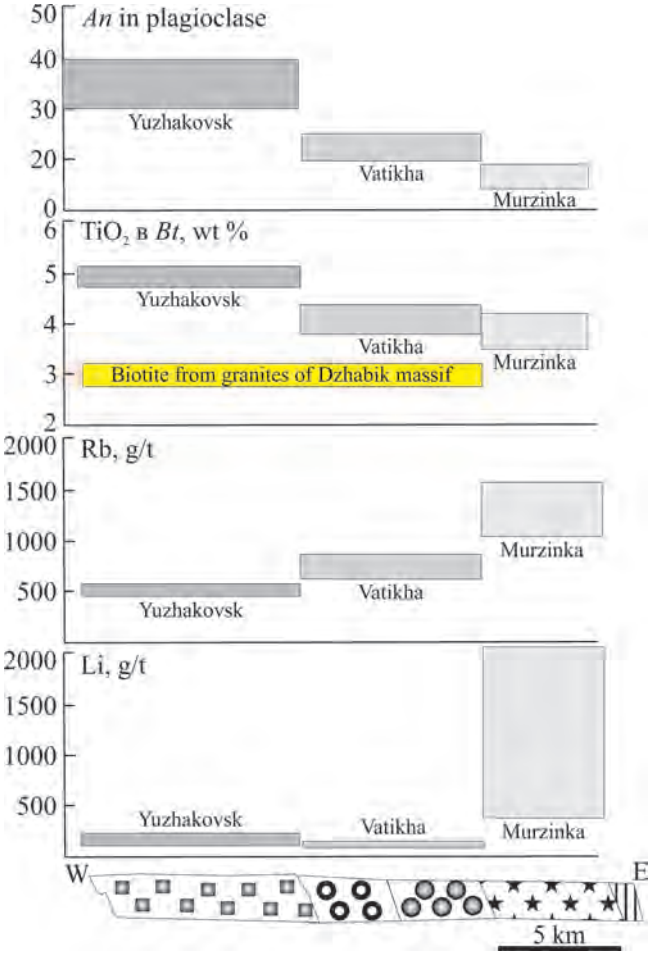

Fig. 8. Content of *An* minal in plagioclase and TiO_2, Rb, Li in the biotite of Yuzhakovo, Vatikha and Murzinka granites.

blendes and plagioclases of gneisses (for the composition of minerals see the monograph [Orogenic granitoid magmatism..., 1994]) are in equilibrium at a pressure of 5–6 kbar [Fershtater, 1990; Molina et al., 2015] and a temperature of 750–800°C. In the eastern direction, the rocks change their composition from predominantly basic to granitoid as they approach the massif. The gneisses of the granitoid composition experienced a high degree of melting; the anatectic melt formed the western part of the Murzinka massif; the gneisses remained mainly in the form of restites in Vatikha granites.

The rocks of the Yuzhakovo complex form a system comprising two generations of veins and small intrusive bodies occurring among gneisses. The granitoids of the first generation are gneissic, whereas the second-generation granitoids are mostly massive; however, gneissic varieties are also noted. All granitoids form intruded bodies, with the contacts with host gneisses being either well-defined or bearing traces of weak granitisation. Different veins have their own orientation of gneissic structures, which indicates the syntectonic nature of the complex.

The rocks of the complex are characterised by a variety of compositions. The rocks of first-generation veins are enriched with calcium and, for the most part, are depleted of potassium and trace elements associated with it; whereas in the second-generation granitoids, the content of potassium and especially rubidium increases. In terms of the content of niobium, lithium, rubidium and the K/Rb ratio, they exhibit the same trends as the granites of the Vatikha and Murzinka complexes that make up the Murzinska massif and are at the beginning of the evolutionary series (see Figures 4–6).

The absence of noticeable migmatisation and the intrusive contacts of the Yuzhakovo granite veins indicate that the zone of magma generation is located below the modern erosional truncation. Considerable variations in the composition of the granitoids of the Yuzhakovo complex, much more significant than in the rocks of the Vatikha and Murzinka complexes, are evidently caused by fluctuations in the degree of partial melting and the composition of the gneiss protolith.

The granites of the Vatikha and Murzinka complexes make up the western and eastern parts of the Murzinska massif, respectively. In the endocontact zone reaching up to 1–1.5 km in width, Vatikha granites contain the inclusions of granodiorite and adamellite composition, which constitute variously transformed restites of a granite-gneiss substrate. These granites, identified as the West Vatikha subcomplex, are close in terms of their chemical composition and mineralogy to Yuzhakovo granites. To the east, they gradually become enriched with rubidium, lithium and niobium (East Vatikha subcomplex) and, by all indications, exhibit similarities with the granites of the Murzinska complex. The granites of the Vatikha complex possess distinctive 'crustal' isotopic characteristics, while the Murzinska granites are very different in their low content of radiogenic strontium and near-zero εNd_{255} values. Considering that granites are of the same isotopic age, these data clearly indicate different substrates for Vatikha and Murzinka granites. The presence in the former of numerous granite gneiss inclusions explains the isotopic parameters of granites by the fact that Proterozoic granite-gneisses constituted their substrate, whereas the isotopic parameters of Murzinka granites and their spatial proximity to Paleozoic sedimentary-volcanic strata indicate that the rocks of the newly formed crust of the orogen – common for most Ural granites – served as the granite protolith [Fershtater, 2013].

All granites constitute crystallised cotectic melt and exhibit corresponding trends in the coordinates K_2O–CaO–Na_2O (Fig. 9a), which is an important petrochemical confirmation of their magmatic origin [Shteinberg, 1985; Fershtater, 1987]. The cotectic range of granites of the Yuzhakovo complex is characterised by the highest CaO content, with that of the Murzinka complex showing the smallest content. Based on the po-

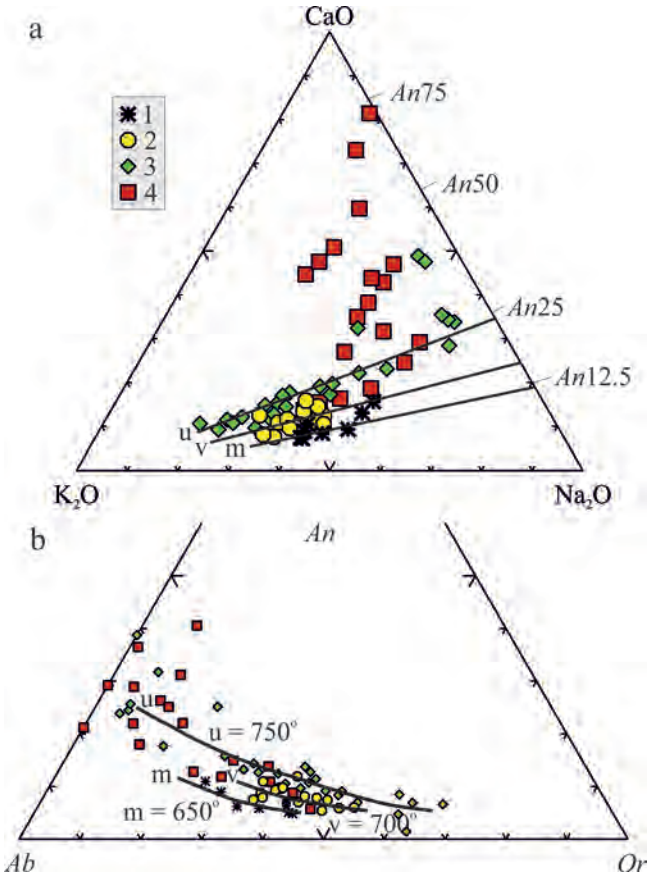

Fig. 9. K_2O–CaO–Na_2O (a) and *Ab–An–Or* (b) diagrams for granitoids and metamorphic rocks.

1–3 – granitoid complexes: 1 – Murzinka, 2 – Vatikha, 3 – Yuzhakovo; 4 – gneisses.
Letters m, v, u denote trends of the corresponding complexes. In diagram b, these trends correspond to the isotherms of ternary feldspars [Ribbe, 1975, and references in this work]. Note a clear decrease in An content of normative plagioclase from the Yuzhakovo to Murzinka complexes, which was mentioned previously and is evidenced by the direct measurements of plagioclase composition (see Fig. 8). The normative amount of *Ab*, *An*, *Or* is compliant with the mesonorms (normative compositions with biotite and amphibole instead of anhydrous iron-magnesium silicates).

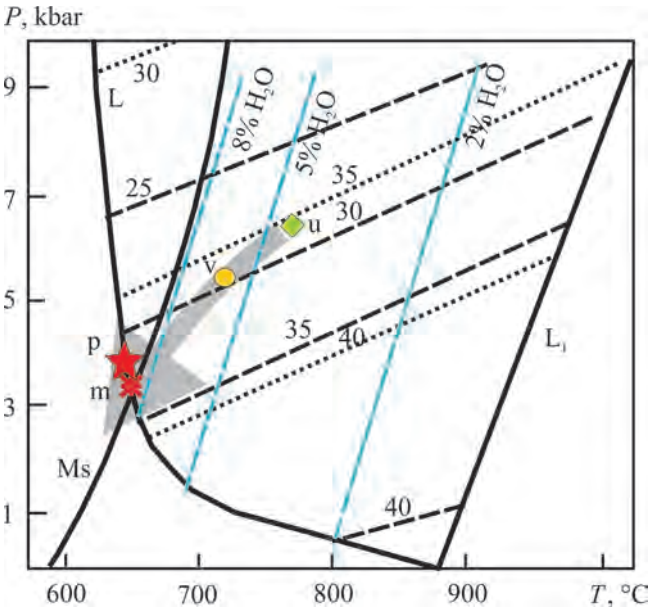

Fig. 10. *T* versus *P* for granitoids. For the principle of plotting and data sources see [Fershtater, 1987, Fig. 33].

The position of the water-saturated (L) and dry (L_1) liquiduses of the system *Ab–Q–Or*–H_2O and also liquidus lines (blue dases) for water contents of 2, 5 and 8 wt % is specified according to [Johannes, Holtz, 1996; Holtz et al., 2001]. The dashed lines having indices 40, 35, 30, 25 denote the quartz content in the ternary minimum of the system *Ab–Q–Or*; the dashed line represents the same in the system *Ab–Q–Or–An* at *An*/(*An* + *Ab* + *Or*) = 0.05. Their position is also specified according to the above-mentioned authors. The average contents of quartz in granites of the Yuzhakovo (u), Vatikha (w) and Murzinka (m) complexes are calculated using mesonorms according to the data from Tables 4 and 5; whereas the average contents of quartz in the graphic pegmatite from Mokrusha vein (p) were determined on the basis of calculations carried out in thin sections; the temperatures are taken from Fig. 9b. *Ms* – stability curve of muscovite in granite [Huang, Willie, 1973]. Other explanations are given in the text.

sition of the imaging points of granites from different complexes in the Ab – An – Or diagram (Fig. 9b), considering the known data on the temperature dependences of feldspar compositions [Ribbe, 1975, and references in this work], we can approximately estimate their crystallisation temperature, which drops from 750°C for granites of the Yuzhakovo complex to 650°C for granites of the Murzinka complex. The presence of antiperthite plagioclases in Yuzhakovo and Vatikha granites serves as the mineralogical verification of the given numbers. The use of such an indicator of the order of crystallisation as the fluorine content in apatite inclusions in rock-forming minerals [Fershtater, 1987] provides additional confirmation of granite composition conforming with granite eutectics. The data presented below indicate a constant fluorine content (2.35–2.95%) in apatite inclusions from all the main minerals of typical granite (samples 44) of the Murzinka complex, which is a consequence of their simultaneous (eutectic) crystallisation from the melt. The fluorine content exceeds 3% only in the late intergranular apatite and the apatite inclusions in the late muscovite replacing biotite. *The fluorine content (wt %) in apatite included in*: plagioclase – 2.35, biotite – 2.48, orthoclase – 2.66, quartz – 2.95, muscovite 1 – 2.57, muscovite 2 – 3.43, intergranular – 3.77.

The *P–T*–H_2O parameters characterising the evolution of granite magmatism are shown in Figure 10. The evolutionary trend indicates a regular change in the P-T parameters in the granitoid complexes of the latitudinal cross section of the massif, i.e. from its bottom to the top, from the granitoids of the Yuzhakovo complex to

Murzinka granites. The pressure during the separation of the eutectic granite melt, in this case, varies from 6–7 to 3 kbar, with the water content in the melt increasing from 4–5 to 8 wt %. Murzinka granites are on the aqueous liquidus of granite near the stability curve of muscovite in a granite melt, which is consistent with the two-mica composition of granites.

The melt filled the fault zone at the border of the pre-Paleozoic basement in the west and the newly formed crust composed of Silurian and Devonian volcanic-sedimentary rocks in the east, mainly via the dyke filling mechanism [Petford et al., 1993], as evidenced by the subvertical form of Vatikha and Murzinka granites differing in structure and composition [Orogenic granitoid magmatism..., 1994]. The specified features of the Murzinka massif are to some extent characteristic of the majority of Permian granite massifs of the paleocontinental zone (northwestern megablock) and distinguish them from the granites of the Kochkar anticlinorium, where the uniformly aged granites of the paleocontinental zone (southeast megablock) are most clearly represented [Fershtater, 2013]. Massifs of the latter are confined to dome structures and are formed as a result of diapirism combined with the mechanism of fracture development [Clemens, Mawer, 1992].

In such massifs, separate granite bodies differing in structure and composition form mostly flat deposits [Fershtater, Borodina, 1975].

There is also an issue concerning the nature of the pegmatites of the Ural gemstone belt, which developed within the MMC. The performed studies indicate clear geochemical differences between the chamber pegmatites of the gemstone belt and various pegmatites associated with the granites of the Yuzhakovo, Vatikha and Murzinka complexes. Chamber pegmatites of the gemstone belt occurring in the Proterozoic gneisses constitute a separate episode of magmatism, which according to preliminary data (K-Ar age) completed granite formation in the region and was not directly related to the formation of the Murzinka massif.

The work was carried out within project No. 0393-2016-0020 of the state task of the IGG UB RAS, state registration number AAAA-A18-118052590029-6.

REFERENCES

Borshchov S.K., Fershtater G.B. (2017) The self-colored belt of the Urals: Alabash ore field, vein Mokrusha. *Putevoditel' Sredneural'skoi polevoi ekskursii. "Granity i evolyutsiya Zemli*". III Mezhdunar. geol. konf. [Guide of Sredneuralskaya field trip. III Intern. Geol. Conf. "Granites and the evolution of the Earth"]. Ekaterinburg, IGG UrO RAN Publ., 27-37. (In Russian)

Clemens J.D., Mawer C.K. (1992) Granite magma transport by fracture propagation. *Tectonophysics*, **204**(3-4). 331-360.

Couzinie S., Moyen J.-F., Villaros A.,Paquette J.-L., Scarrow J.H., Marignac C. (2014) Temporal relatioships between Mg-K mafic magmatism and catastrophic melting of the Variscan crust in the southern part of Velay Complex (Massif Central, France). *J. Geosci*., **59**, 69-86.

Fershtater G.B. (1987) *Petrologiya glavnykh intruzivnykh assotsiatsii* [Petrology of the main intrusive associations]. Moscow, Nauka Publ., 232 p. (In Russian)

Fershtater G.B. (1990) Empirical plagioclase-hornblende barometer. *Geokhimiya*, (3), 328-335.

Fershtater G.B. (2013) *Paleozoiskii intruzivnyi magmatizm Srednego i Yuzhnogo Urala* [Paleozoic intrusive magmatism of the Middle and Southern Urals]. Ekaterinburg, UrO RAN Publ., 365 p. (In Russian)

Fershtater G.B., Borodina N.S. (1975) *Petrologiya magmaticheskikh granitoidov* [Petrology of magmatic granitoids]. Moscow, Nauka Publ., 287 p. (In Russian)

Fersman A.E. (1940) *Pegmatity* [Pegmatites]. Moscow, AN SSSR Publ., 712 p. (In Russian)

Gerdes A., Montero P., Bea F., Fershtater G., Borodina N., Osipova T., Shardakova G. (2002) Peraluminous granites frequently with mantle-like isotope compositions: the continental-type Murzinka and Dzhabyk batholith of the eastern Urals. *Intern. J. Earth Sci. (Geol. Rundsch.)*, **91**, 3-19.

Holtz F., Becker A., Freise M., Johannes W. (2001) The water-saturated and dry Qz–Ab–Or system revised. Experimental results of very low water activities and geological implications. *Contrib. Mineral. Petrtol*., **141**, 347-357.

Huang W.L., Willie R.J. (1973) Melting relations of muscovite granite to 35 kbar as a model for fusion of metamorphosed subducted oceanic sediments. *Contrib. Mineral. Petrtol*., 42, 1-14.

Johannes W., Holtz F. (1996) Petrogenesis and experimental petrology of granitic rocks. Springer, Berlin, Heidelberg, New York., 336 p.

Keil'man G.A. (1974) *Migmatitovye kompleksy podvizhnykh poyasov* [Migmatitic complexes of mobile belts]. Moscow, Nedra Publ., 200 p. (In Russian)

Korovko A.V., Dvoeglazov D.A. (1986) Geological position and internal structure of the Murzinka metamorphic complex. *Korrelyatsiya i kartirovanie magmaticheskikh i metamorficheskikh kompleksov Urala* [Correlation and mapping of magmatic and metamorphic complexes of the Urals]. Sverdlovsk, IGG UrO RAN Publ.,73-75. (In Russian)

Krasnobaev A.A., Bea F., Fershtater G.B., Montero P. (2005) Zircon geochronology of the murzinka metamorphic complex (Middle Urals). *Dokl. Akad. Nauk.*, **404**(3), 407-410. (In Russian)

Le Maitre R.W. (ed.). (1989) A Classification of Igneous Rocks and Glossary of Terms. Blackwell, Oxford, 193 pp.

Levin V.Ya., Koroteev V.A, Zvonareva G.K. (1975) Corundum syenites from Yubileynaya mine. *Materialy k mineralogii Urala* [Materials to the mineralogy of the Urals]. Tr. Ilmensk. gos. zapovednik, 44-49. (In Russian)

Molina J. F., Moreno J.A., Castro A., Rodriguez, Fershtater G.B. (2015) Calcic amphibole thermobarometry in metamorphic and igneous rocks: New calibrations based on plagioclase/amphibole Al-Si partitioning and amphibole/liquid Mg partitioning. *Lithos.*, **232**, 286-305.

Montero P., Bea F., Gerdes A., Fershtater G.B., Osipova T.A., Borodina N.S., Zinkova E.A. (2000) Single-zircon evaporation ages and Rb-Sr dating of four major Variscan batholiths of the Urals. A perspective on the timing of deformation and granite generation *Tectonophysics*, **317**, 93-108.

Muller A., Romer R.L., Pedersen R.-B. (2017) The sveconorvegian pegmatite province – thousands of pegmatites without parental granites. *Canad. Mineral.*, **55**, 283-315.

Orogennyi granitoidnyi magmatizm Urala [Orogenic granitoid magmatism of the Urals]. (Ed. G.B. Fershteter). (1994) Miass, IGG UrO RAN Publ., 250 p. (In Russian)

Petford N., Kerr C.R., Lister R.G. (1993) Dike transport of granitoid magmas. *Geology*, **21**, 845-848.

Popov V.A., Popova V.I. (1975) To the mechanism for the formation of feldspar glasses around corundum crystals, "Yubileynaya" mine in the Ilmeny mountains *Materialy k mineralogii Urala* [Materials to the mineralogy of the Urals]. Tr. Ilmensk. gos. zapovednik, 50-57. (In Russian)

Ribbe P.H. (1975) Feldspar mineralogy: short course notes. (Ed. P.H. Ribbe). Blacksburg, Amer. Miner. Soc. Southern print. Co., **2**, 1-52.

Sabatier H. (1980) Vaugnerites and granites, a peculiar association of basic and acid rocks. *Bull. Mineral.*, **103**, 507-522.

Sabatier H. (1991) Vaugnerites: special lamprophyre-derived mafic enclaves in some Hercynian granites from Western and Central Europe. *Enclaves and granite petrology*. (Eds J. Didier, B. Barbarin). Elsevier, Amsterdam, 63-81.

Scarrow J.H., Molina J., Bea F., Montero P. (2009) Within-plate calc-alkaline rocks: insights from alkaline mafic magmas – peraluminous crustal melt hybrid appinites of the Central Iberian Variscan continental collision. *Lithos.*, **110**, 50-64.

Shteinberg D.S. (1985) *O classifikatsii magmatitov* [On the classification of magmatites]. Moscow, Nauka Publ., 159 p. (In Russian).

Talantsev A.S. (1988) *Kamernye pegmatity Urala* [Chamber pegmatites of the Urals]. Moscow, Nauka Publ., 144 p. (In Russian)

Winchester J.A., Floyd P.A. (1977) Geochemical discrimination of different magma series and their differentiation products using immobile elements. *Chem. Geol.*, **20**, 325-343.